Communication

Coexistence and Coupling of Two Distinct Charge Density Waves in SmTe

Christos D. Malliakas, Maria Iavarone, Jan Fedor, and Mercouri G. Kanatzidis

J. Am. Chem. Soc., **2008**, 130 (11), 3310-3312 • DOI: 10.1021/ja7111405

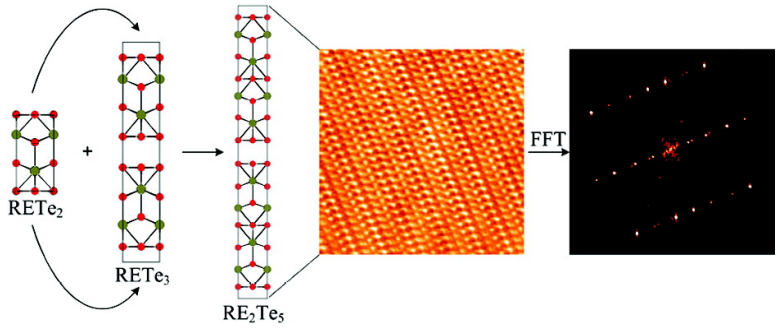

More About This Article

Additional resources and features associated with this article are available within the HTML version:

- Supporting Information
- Links to the 1 articles that cite this article, as of the time of this article download
- Access to high resolution figures
- Links to articles and content related to this article
- Copyright permission to reproduce figures and/or text from this article

View the Full Text HTML

J|A|C|S
COMMUNICATIONS

Published on Web 02/21/2008

Coexistence and Coupling of Two Distinct Charge Density Waves in Sm_2Te_5

Christos D. Malliakas,[†,‡] Maria Iavarone,[§] Jan Fedor,[§] and Mercouri G. Kanatzidis*[,‡,§]

Department of Chemistry, Michigan State University, East Lansing, Michigan 48824, Department of Chemistry, Northwestern University, Evanston, Illinois 60208, and Materials Science Division, Argonne National Laboratory, Argonne, Illinois 60439

Received December 15, 2007; E-mail: m-kanatzidis@northwestern.edu

Low-dimensional systems often exhibit electronic instabilities that can lead to charge density waves (CDWs) or superconductivity. The CDWs have a characteristic frequency q (q-vector) that corresponds to the so-called nesting vector of the Fermi surface (FS). Nesting favors electron−phonon coupling, which is believed to be responsible for the formation of the CDW and often overpowers a competing superconductive state. Although the description of CDW behavior for one-dimensional systems (1D) is well established, no proper theoretical models have been developed for the two-dimensional (2D) cases.[1]

Recent studies have focused on the high-temperature CDW family of materials RETe$_2$ and RETe$_3$ (RE = rare earth element) which contain square Te nets. We now have new insights as to the nature of the phenomenon in these materials.[2−4] The RETe$_3$ family has gained more attention in recent years because of its quasi-2D incommensurate CDW states and their effect on the electronic structure. Extensive structural,[5] spectroscopic,[6] and other physical[7] studies have revealed unique chemical and physical behavior among the classical CDW systems. However, only recently was it recognized through angle-resolved photoemission spectroscopy (ARPES) studies that LaTe$_2$ is the first semiconductor where the 2D CDW distortion is Fermi surface nesting driven.[8] Variations in the electron count alters the energy of the Fermi level and thus the nesting properties of the Fermi surface (q-vector). The average formal charge per Te atom in the Te net of RETe$_3$ is −0.5e whereas for RETe$_2$ is −1e. Based on these results, it is compelling to examine the family RE_2Te$_5$, in which the types of square Te nets found in RETe$_2$ and RETe$_3$ now occur together in the same lattice. Each has its own average oxidation state of 1- and 1/2- respectively. The electronic behavior of such a hybrid system is unknown. Surprisingly, only a few physical and structural characterization studies for RE_2Te$_5$ have been reported.[9] Will these two nets act independently to create their own CDW or would a single emergent CDW behavior be operative?

The structure of RE_2Te$_5$ is essentially a 1:1 combination of the structures of RETe$_2$ and RETe$_3$, Figure 1. It contains one square net of Te^{1-} atoms found in the RETe$_2$ family and two square nets of Te$^{1/2-}$ atoms present in the RETe$_3$ compound. It is well-known that the number of electrons per Te atom controls the type of CDW modulation.[10] Although the CDW RETe$_2$ and RETe$_3$ compounds are substructure components of the RE_2Te$_5$ phase, no CDW distortions have been found for the composite structure.[9] Here, we report for the first time the structural determination of the incommensurate CDW states in Sm_2Te_5 and confirm the existence of two coexisting CDW states in a single material.

We find that each of the two types of planar Te nets has its own CDW distortion manifested by the existence of two individual

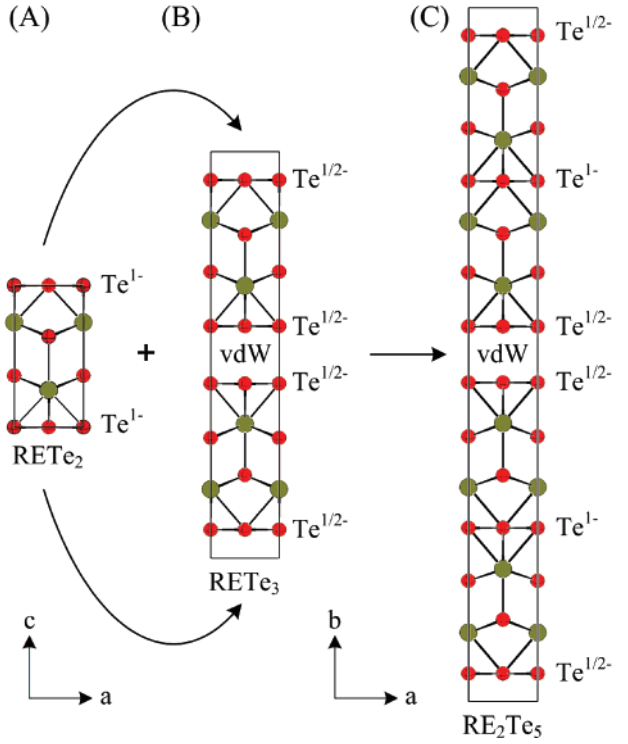

Figure 1. (A) Average structure of RETe$_2$ (Cu$_2$Sb-type) with square nets of Te^{1-}. (B) Average layered structure of RETe$_3$ (NdTe$_3$-type) with square nets of Te$^{1/2-}$. (C) Hybrid average layered structure of RE_2Te$_5$ (Nd$_2$Te$_5$-type) with square nets of both Te^{1-} and Te$^{1/2-}$. The van der Waals (vdW) gaps are indicated.

q-vectors in the structure. We have verified the two CDW modulations by direct visualization of the distortions with scanning tunneling microscopy (STM). The independent character of the two q-vectors was examined with high-temperature single-crystal X-ray diffraction experiments going above the CDW transition.

The RETe$_2$ structure adopts the Cu$_2$Sb structure type where a [RETe]$^+$ sublayer is sandwiched between two square Te^{1-} nets, Figure 1A. The RETe$_3$ structure is NdTe$_3$-type and has a [RETe]$^+$ sublayer sandwiched between two square Te$^{1/2-}$ nets. The RETe$_3$ slabs stack along the b-axis creating van der Waals gaps, Figure 1B. The RE_2Te$_5$ structure is layered and forms by fusing two RETe$_3$ slabs so that a square net of Te^{1-} atoms is created in the middle of now thicker RE_2Te$_5$ slabs. The outer surfaces of this thicker slab are made by planar nets of Te$^{1/2-}$ atoms, Figure 1C. The slabs then stack along the b-axis creating van der Waals gaps (*Cmcm* Nd$_2$Te$_5$ structure type), Figure 1C. The formula can be expressly written as ([RETe]$^+$)$_2$([Te]$^{1/2-}$)$_2$[Te]$^{1-}$. Each RE^{3+} atom is surrounded by nine Te atoms in a monocapped tetragonal antiprismatic geometry. The apparent Te−Te distance in the square nets of Sm_2Te_5 is 3.0715(4) Å for both Te$^{1/2-}$ and Te^{1-} nets at 100 K.

[†] Michigan State University.
[‡] Northwestern University.
[§] Argonne National Laboratory.

10.1021/ja7111405 CCC: $40.75

We find that the Te^{1-} net in the middle of the Sm_2Te_5 slab in fact has vacancies that long range order making $Sm_2Te_{4.90(1)}$ the first rare-earth polytelluride compound with ordered vacancies.[11] Hypostoichiometry is known in the REQ_{2-x} (Q = S,[12] Se,[13] Te[14]) family.

Two CDWs were found in Sm_2Te_5 that create a (3 + 2)-dimensional modulated incommensurate superstructure with two q-vectors at 100 K. A superspace crystallographic approach was necessary to solve the structure.[11] A stable refinement was achieved with $P1(\alpha_1\beta_1\gamma_1,\alpha_2\beta_2\gamma_2)0$ superspace group. The two vectors are $q_1 = 0.3124(3)b^* + 1/2c^*$ and the weaker $q_2 = 0.3303(3)a^* + 0.3315(3)b^* + 0.349(1)c^*$ at 100 K. The temperature dependence of the q-vectors of Sm_2Te_{5-x} surprisingly shows a different trend from the one observed for $SmTe_3$[5c] and $SmTe_2$.[15] The length of the q_1-vector increases to 0.3233(8) at 450 K and the diagonal q_2-vector decreases to $0.3100(8)a^* + 0.3268(8)b^* + 0.345(5)c^*$. At 500 K, the q_1 disappears and q_2 becomes shorter $0.315(1)a^* + 0.315(1)b^* + 351(6)c^*$.

The structural patterns of Te atoms imposed by the CDWs in the square nets of Sm_2Te_5 feature a rich variety of $[Te_n]^{x-}$ oligomers. These are of different length, geometry, and sequence from the ones observed in the corresponding $RETe_3$ family. Some similarities may be found in the parent substructures $SmTe_3$[5c] and $SmTe_2$,[16] but the combination of the two q-vectors and the presence of occupational waves of vacancies create unique Te patterns. The majority of oligomers in the $Te^{1/2-}$ net at 100 K are V-shaped trimers and occasionally N-shaped tetramers, Figure 2A. The main difference from $RETe_3$ though is the discontinuation of the same type of oligomers along the a-axis. Specifically, the sequence of trimers along a-axis now contains tetramers, dimers, and sometimes even single Te atoms (shown with arrows in Figure 2A). The Te−Te length distribution in $Te^{1/2-}$ at 100 K varies from a minimum of 2.933(10) Å and maximum 3.208(10) Å with an average of 3.089(10) Å.

The Te^{1-} net at 100 K contains square-like octamers with a vacancy in the center. Furthermore, different sequence of dimers, V-shaped and linear trimers, L- and T-shaped tetramers, V-shaped pentamers, F-shaped hexamers, and defected square-like heptamers is observed due to vacancy ordering, Figure 2B. The minimum Te−Te bond length in the Te^{1-} net at 100 K is 2.805(19) Å, and it is the shortest observed in the rare-earth polytelluride family. The maximum distance is 3.351(19) Å with an average of 3.083(19) Å.

Both Te nets remain distorted even above the first CDW transition temperature. The existence of the diagonal modulation vector creates distorted patterns with different sequence of oligomers. At 500 K, the $Te^{1/2-}$ pattern consists mainly of alternating N-shaped tetramers and dimers, Figure 2C. The majority of dimers are aligned diagonally in single chains and occasionally in double chains. The bond length distribution becomes very narrow with a minimum of 3.063(5) Å, maximum 3.098(5) Å and an average of 3.095(5) Å. The Te^{1-} net at 500 K does not show any of the square-like octamers but it contains sequence of monomers, dimers, V-shaped trimers, Z- and C-shaped pentamers with a linear Te atom, Figure 2D. The minimum Te−Te bond is 2.953(10) Å, the maximum 3.211(11) Å with an average distance of 3.085(11) Å.

STM has been used widely to study CDW modulations with atomic resolution in direct space.[17] To verify the presence of two different CDW distortions in the $Te^{1/2-}$ net of Sm_2Te_5, we performed a low-temperature STM (LT-STM) study.[18] The STM experiment undertaken at 4.2 K clearly shows an incommensurate CDW with wave vector in the $Te^{1/2-}$ plane along the diagonal of the Te−Te square net. The wave vector measured by Fourier transform of the STM topography images is in agreement with diffraction data. The CDW pattern revealed in Sm_2Te_5 is similar to the one observed in $RETe_3$.[5b,19] However, an additional wave vector along the Te−Te bond was observed in Sm_2Te_5. The STM image of the Sm_2Te_5 surface is shown in Figure 3A, evidencing the distorted Te net with in-plane lattice parameter $a = 3.1(2)$ Å. The fast Fourier transform (FFT) analysis of the STM image is shown in Figure 3B. The peaks L originate from the Te square lattice. The line profile cut from O to A, along the diagonal of the Te square net, is shown in Figure 3C. This profile shows five peaks, one corresponding to the superlattice $2\pi/a$ and four intermediate peaks at 0.31, 0.38, 0.62, and 0.69. We identify $q_1 = 0.31$ as the CDW wave vector and the other peaks as the $1 - 2q_1$, $2q_1$, $1 - q_1$ harmonics respectively. The line profile cut OL, in Figure 3D, shows two additional peaks corresponding to the wave vector $q_2 = 0.33$ and to the harmonic $2q_2 = 0.66$ in the direction of the Te−Te bond. The intensity of the wave vector q_2 is weaker compared to q_1 consistent to what has been observed from diffraction measurements.

The Sm_2Te_5 shows a metallic behavior since the CDW does not remove all the states from the Fermi level.[9b] Because of the poor metallic character we observed spectroscopically electronic transitions associated with the energy gap, Figure 3E. The data showed a transition ~0.17 eV that is higher in energy from the corresponding transition of ~0.13 eV in $SmTe_3$. The energy gap difference is consistent with the higher CDW transition temperature of Sm_2Te_5 (>450 K) compared to $SmTe_3$ (~420 K).[11]

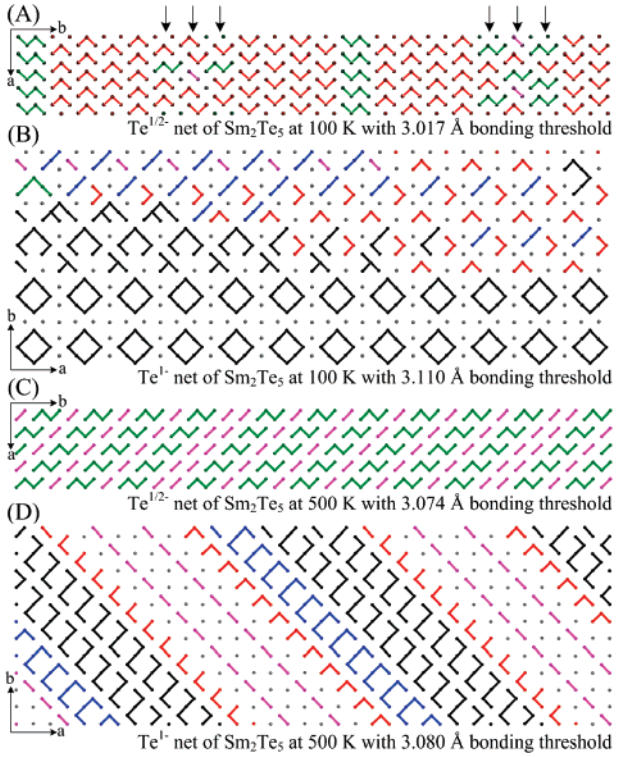

Figure 2. Distorted tellurium nets of Sm_2Te_5 at two different temperatures above and below the first T_{CDW}. (A) $Te^{1/2-}$ net at 100 K and a threshold of 3.017 Å. Different sequence of oligomers along a-axis is indicated with arrows. (B) Te^{1-} net at 100 K with a bonding threshold of 3.110 Å and occupational cutoff at 80%. (C) $Te^{1/2-}$ net at 500 K and a threshold of 3.070 Å. (D) Te^{1-} net at 500 K with a bonding threshold of 3.090 Å and occupational cutoff at 80%. Its bonding threshold value corresponds to the maximum value at which the trimers, tetramers, and other oligomers with less than five atoms (except square-like fragments) are not interconnected. A more extended region of the distorted Te nets can be found in the Supporting Information.

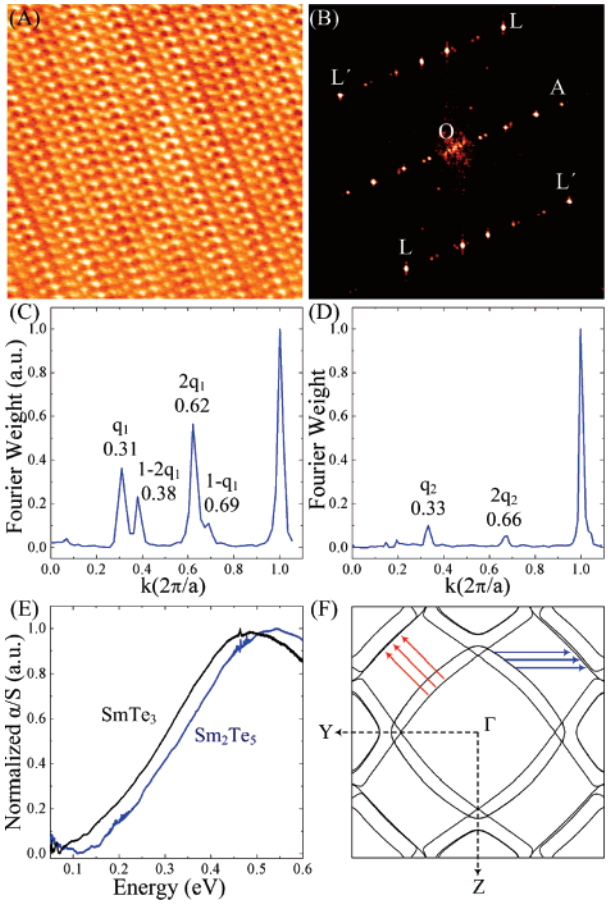

Figure 3. (A) STM image of the Sm_2Te_5 surface of $Te^{-1/2}$. The scanning area was 92.5 Å^2, the tunneling current 20 pA, and the voltage +0.2 V. (B) 2D-FFT of the STM image reported in 3A. The peaks L correspond to the Te square lattice. (C) Line cut plot from O to A, along the diagonal of the Te square net. (D) Line cut plot from O to L. (E) Room temperature infrared absorption spectrum of Sm_2Te_5 and $SmTe_3$ single crystals. Energy gap at ~0.17 eV corresponds to Sm_2Te_5 and ~0.13 eV to $SmTe_3$. (F) Calculated Fermi surface topology of La_2Te_5. Possible nesting vectors with an average length of $q_1 = 0.32(2)$ along the b^* axis (Y point) are drawn in blue arrows and $q_2 = 0.35(2)$ along the diagonal are drawn in red arrows.

Electronic band structure calculations at the density functional theory (DFT) level[20] performed on the undistorted (no CDW and vacancy ordering) structure of La_2Te_5. The most important feature of the FS of La_2Te_5 is the separation between the two bands located in the center of the FS (Γ point), Figure 3F. These are Te *p* bands in character coming from the two Te nets with different oxidation states. The separation of the bands is such that the topology of the FS favors the formation of two nesting vectors. One vector along the b^* director with a length of 0.32(2) and a second vector along the diagonal of a^*-b^* plane at 0.35(2).[21] A weaker splitting of bands was found for the *RE*Te_3 in respect to the *RE*Te_2 due to the interactions between the Te layers separated by the van der Waals gap.[22] Although the distance of the Te bilayers separated by the van der Waals gap is essentially the same in both $SmTe_3$ and Sm_2Te_5, the presence of the additional Te^{1-} layer seems strongly to affect the nesting properties of the FS. The nesting vector from 0.28(2) for $LaTe_3$ increases significantly to 0.32(2) for La_2Te_5 in a similar fashion observed for $KCuLaTe_4$.[23]

Two distinct CDW distortions exist in the intergrowth Sm_2Te_5 compound with some hybrid character coming from the coupling of two individual *q*-vectors. The *RE*$_2Te_5$ family represents a rare example of composite structures that possess two Te nets with different oxidation states, $Te^{1/2-}$ and Te^{1-}. In combination with occupational modulation waves of vacancies, the new distorted Te patterns surprisingly are very different from the ones found in the two parent substructures. The new phenomena reported here provide valuable structural details and physical properties to the developing theory of two-dimensional CDW systems. Detailed structural examination of other *RE*Te_2 and *RE*$_2Te_5$ members is in progress to elucidate and compare their CDW distortions.

Acknowledgment. Support from the NSF (DMR-0801855, FRG-0703882) is gratefully acknowledged. The STM work was supported by UChicago Argonne, LLC, Operator of Argonne National Laboratory ("Argonne"). Argonne, a U.S. Department of Energy Office of Science laboratory, is operated under Contract No. DE-AC02-06CH11357.

Supporting Information Available: Details of structural analysis, DFT calculations, and CIF files. This material is available free of charge via the Internet at http://pubs.acs.org.

References

(1) Grüner, G. *Density Waves in Solids*; Addison-Wesley: Reading, MA, 1994.
(2) Min, B. H.; Cho, J. H.; Lee, H. J.; Han, C. W.; Kim, D. L.; Kwon, Y. S. *Phys. B* **2000**, *281*, 118.
(3) Kwon, Y. S.; Min, B. H. *Phys. B* **2000**, *281*, 120.
(4) Shin, Y. S.; Han, C. W.; Min, B. H.; Lee, H. J.; Choi, C. H.; Kim, Y. S.; Kim, D. L.; Kwon, Y. S. *Phys. B* **2000**, *291*, 225.
(5) (a) Malliakas, C.; Billinge, S. J. L.; Kim, H. J.; Kanatzidis, M. G. *J. Am. Chem. Soc.* **2005**, *127*, 6510. (b) Kim, H. J.; Malliakas, C. D.; Tomic, A.; Tessmer, S. H.; Kanatzidis, M. G.; Billinge, S. J. L. *Phys. Rev. Lett.* **2006**, *96*, 226401. (c) Malliakas, C. D.; Kanatzidis, M. G. *J. Am. Chem. Soc.* **2006**, *128*, 12612.
(6) Gweon, G. -H.; Denlinger, J. D.; Clack, J. A.; Allen, J. W.; Olson, C. G.; DiMasi, E. D.; Aronson, M. C.; Foran, B.; Lee, S. *Phys. Rev. Lett.* **1998**, *81*, 886.
(7) (a) Iyeiri, Y.; Okumura, T.; Michioka, C.; Suzuki, K. *Phys. Rev. B* **2003**, *67*, 144417. (b) Ru, N.; Fisher, I. R. *Phys. Rev. B* **2006**, *73*, 033101.
(8) Garcia, D. R.; Gweon, G. -H.; Zhou, S. Y.; Graf, J.; Jozwiak, C. M.; Jung, M. H.; Kwon, Y. S.; Lanzara, A. *Phys. Rev. Lett.* **2007**, *98*, 166403.
(9) (a) Pardo, M. P.; Flahaut, J. *Bull. Soc. Chim.* **1967**, *10*, 3658. (b) DiMasi, E.; Foran, B.; Aronson, M. C.; Lee, S. *Chem. Mater.* **1994**, *6*, 1867.
(10) Patschke, R.; Kanatzidis, M. G. *Phys. Chem. Chem. Phys.* **2002**, *4*, 3266.
(11) Details can be found in the Supporting Information.
(12) Plambeck-Fischer, P.; Abriel, W.; Urland, W. *J. Solid State Chem.* **1989**, *78*, 164.
(13) Grupe, M.; Urland, W. *J. Less-Common Met.* **1991**, *170*, 271.
(14) Domange, L.; Flahaut, J.; Pardo, M. P.; Chirazi, A. N.; Guittard, M. *C. R. Acad. Sci.* **1960**, *250*, 857.
(15) Preliminary results of superspace analysis on $SmTe_{1.86(1)}$ gave a tetragonal unit cell with $a = 4.3520(3)$ Å, $c = 8.9451(7)$ Å and two *q*-vectors of $q_1 = 0.2965(3)a^* + 0.2965(3)b^* + 1/2c^*$ and $q_2 = 0.2965(3)a^* - 0.2965(3)b^* + 1/2c^*$ at 100 K. The q-vector dependence at high temperature (500 K) is negligible with cell parameters $a = 4.3787(4)$ Å, $c = 8.9976(7)$ Å and $q_1 = 0.2974(3)a^* + 0.2974(3)b^* + 1/2c^*$ and $q_2 = 0.2974(3)a^* - 0.2974(3)b^* + 1/2c^*$. The stoichiometry of the compound was determined crystallographically from the refinement of the subcell reflections.
(16) (a) Park, S. -M.; Park, S. -J.; Kim, S. −J. *J. Solid State Chem.* **1998**, *140*, 300. (b) Ijjaali, I.; Ibers, J. A. *J. Solid State Chem.* **2006**, *179*, 3456.
(17) Coleman, R. V.; Dai, Z.; McNairy, W. W.; Slough, C. G.; Wang, C. In *Scanning Tunneling Microscopy*; Stroscio, J. A., Kaiser, W. J., Eds; Academic: San Diego, 1993.
(18) STM measurements were performed with a low temperature home made STM at 4.2 K. The samples were cleaved under inert atmosphere and quickly cooled down at 4.2 K. Considering that the cleavage occurs between the van der Waals gap we expect the topmost layer, observable with the STM, to be the $Te^{1/2-}$ net. Topography images were acquired in constant current mode as well as in constant height mode and at different voltage tip-sample.
(19) Fang, A.; Ru, N.; Fisher, I. R.; Kapitulnik, A. *Phys. Rev. Lett.* **2007**, *99*, 046401.
(20) (a) Hohenberg, P.; Kohn, W. *Phys. Rev.* **1964**, *136*, B864. (b) Kohn, W.; Sham, L. *Phys. Rev.* **1965**, *140*, A1133.
(21) We calculated the average value of 0.32(2) from the minimum value of the nesting vector of 0.30 (close to the Y point) and maximum of 0.34 (close to the Z point).
(22) Laverock, J.; Dugdale, S. B.; Major, Zs.; Alam, M. A; Ru, N; Fisher, I. R.; Santi, G.; Bruno, E. *Phys. Rev B* **1995**, *52*, 14516.
(23) Malliakas, C. D.; Kanatzidis, M. G. *J. Am. Chem. Soc.* **2007**, *129*, 10677.

JA7111405